Title
CREB regulates excitability and the allocation of memory to subsets of neurons in the amygdala.

Journal
Nature neuroscience, 12(11)

ISSN
1097-6256

Authors
Zhou, Yu
Won, Jaejoon
Karlsson, Mikael Guzman
et al.

Publication Date
2009-11-01

DOI
10.1038/nn.2405

Peer reviewed

HHS Public Access

Author manuscript

Nat Neurosci. Author manuscript; available in PMC 2010 May 01.

Published in final edited form as:

Nat Neurosci. 2009 November ; 12(11): 1438–1443. doi:10.1038/nn.2405.

CREB regulates excitability and the allocation of memory to subsets of neurons in the amygdala

Yu Zhou[1,2,3,4], **Jaejoon Won**[1,2,3,4], **Mikael Guzman Karlsson**[1,2,3,4], **Miou Zhou**[1,2,3,4], **Thomas Rogerson**[1,2,3,4], **Balaji J.**[1,2,3,4], **Rachael Neve**[5], **Panayiota Poirazi**[6], and **Alcino J. Silva**[1,2,3,4,*]

[1]Department of Neurobiology, University of California, Los Angeles, California 90095-1761, USA

[2]Semel Institute, University of California, Los Angeles, California 90095-1761, USA

[3]Department of Psychology, University of California, Los Angeles, California 90095-1761, USA

[4]Brain Research Institute, University of California, Los Angeles, California 90095-1761, USA

[5]Picower Institute of MIT, Cambridge, Massachusetts 02138, USA

[6]Computational Biology Laboratory, Institute of Molecular Biology and Biotechnology (IMBB), Foundation of Research and Technology-Hellas (FORTH), Vassilika Vouton, GR 711 10 Heraklion, Crete, Greece

Abstract

The mechanisms that determine how information is allocated to specific regions and cells in the brain are fundamentally important for memory capacity, storage and retrieval, but are poorly understood. Here, we manipulated CREB in a subset of lateral amygdala (LA) neurons with a modified Herpes Simplex Virus (HSV), and reversibly inactivated transfected neurons with the *Drosophila* allatostatin G-protein-coupled receptor (AlstR)/ligand system. We found that inactivation of the HSV-CREB subpopulation of neurons with allatostatin (AL) during training disrupted memory for tone conditioning, while inactivation of a similar proportion of HSV-LacZ control neurons did not. Whole-cell recordings of fluorescently tagged HSV-CREB neurons revealed that neurons with higher CREB levels are more excitable than neighboring neurons, and show larger synaptic efficacy changes following conditioning. Our findings demonstrate that CREB modulates the allocation of fear memory to specific cells in lateral amygdala, and suggest that neuronal excitability plays a key role in this process.

Memory is thought to depend on specific sets of connected neurons, which together support the `memory trace'. Previous results demonstrated that only a portion of eligible neurons within a network participate in a given memory. For example, approximately 70% of lateral amygdala neurons receive the sensory input involved in tone conditioning, but only less than

*Correspondence should be addressed to A.J.S. (silvaa@mednet.ucla.edu).

AUTHOR CONTRIBUTIONS Y.Z., J.W. and A.J.S. designed the experiments. Y.Z., J.W., M.G.K and T.R. carried out the behavioral experiments. Y.Z. performed the patch-clamp and whole-cell recording experiments. J.W. generated the viral vectors and R.N. provided the viral preparations. M.Z. carried out the western blot analysis. Y.Z. and J.W. analyzed the data. B.J. and P.P. helped with the discussion. Y.Z and A.J.S wrote the paper.

25% are thought to encode this form of conditioning1–6. Why are some neurons, rather than their neighbors, recruited in storing a given memory? Recent results suggested that the transcription factor CREB (cyclic adenosine 3′,5′-monophosphate response element-binding protein) plays a crucial role in determining which neurons in lateral amygdala take part in encoding an auditory fear memory: neurons with relatively higher CREB levels are preferentially recruited into fear memory traces5,6. In this study, we used a novel approach, which combines cell specific molecular manipulations with inducible and reversible inactivation of targeted cells, to study the molecular basis of memory allocation in amygdala neurocircuits. At the heart of our approach is the transfection of a subset of neurons in the amygdala with a viral vector that includes a fluorescently tagged *Creb1* gene and a receptor system that allows us to reversibly silence those neurons. We show that the virally manipulated CREB biases the allocation of memory to the transfected neurons, since silencing those neurons has a disproportionate impact on memory. Importantly, we also show that these neurons with higher CREB levels are more excitable than neighboring neurons, and experience larger synaptic efficacy changes following conditioning.

RESULTS

We used a neurotropic, replication-defective Herpes Simplex Virus (HSV)7 to co-express green fluorescent protein (GFP)-tagged CREB and the *Drosophila* allatostatin receptor (AlstR)8 (HSV-CREB virus; Fig. 1a) in a subset of LA neurons. The activation of AlstRs has been shown to turn on endogenous mammalian G-protein-coupled inwardly rectifying K^+ (GIRK) channels. Upon binding to its ligand (allatostatin; AL), AlstR/GIRK complexes cause membrane hyperpolarization and consequently a decrease in neuronal excitability8. Since previous findings showed that there is abundant expression of GIRK channels in the amygdala9, we expected that the activity of HSV-CREB transfected neurons in tone-conditioned mice could be manipulated by local infusion of AL10,11. As a control, we also used a virus that expressed GFP-tagged β-galactosidase (LacZ) instead of GFP-CREB (HSV-LacZ virus; Fig. 1a). These viruses were microinjected into lateral amygdala, which is essential for auditory Pavlovian fear-conditioning9,10.

Histological staining with a GFP antibody revealed that ~20% of lateral amygdala neurons were transfected with either virus and that the majority of transfected cells were within the lateral amygdala (Fig. 1b). No significant difference was observed between the infection rates for HSV-CREB and HSV-LacZ viruses (18 ± 3% versus 21 ± 4%, $n = 4$ mice per group, $P > 0.05$). Cannula placement was confirmed with crystal violet staining at the end of each experiment (supplementary Fig.1). Only those mice with bilateral placements in the basolateral complex of the amygdala were included in analysis. Importantly, western blot analyses showed that HSV-CREB viral transfection increased CREB levels in the amygdala; Transfection with HSV-LacZ had no detectable effect on CREB expression (Supplementary Fig.2).

We first determined whether lateral amygdala neurons transfected with either the HSV-CREB or the HSV-LacZ virus can be selectively silenced by AL administration. Whole-cell patch clamp recordings were performed in both visually identified GFP^+ neurons and GFP^- neighboring cells in the same slices from HSV-CREB or HSV-LacZ mice. Consistent with

previous studies12, we found that AL administration quickly and reversibly caused the membrane potential to become more negative (−5.9 ± 1.2 mV, $t = 3.73$, $P < 0.01$) in GFP^+ neurons, but had no effect on GFP^- neighboring cells (−0.3 ± 0.9 mV). Moreover, AL administration quickly and reversibly increased the spike current threshold (600 ± 210% of the baseline, $t = 2.33$, $P < 0.05$) and decreased the input resistance (51 ± 12% of the baseline, $t = 3.96$, $P < 0.01$) of GFP^+ lateral amygdala neurons, while having no effect on GFP^- neurons (Fig. 1c–e).

Cell-specific disruption of fear memory in HSV-CREB mice

Next, we determined whether inactivation of the subpopulation of lateral amygdala neurons transfected with HSV-CREB disrupted memory for tone conditioning. If higher levels of CREB disproportionally commit transfected neurons to encoding the memory for tone fear conditioning5,6, then inactivation of these neurons should have a much greater effect on recall than inactivation of neurons transfected with the control HSV-LacZ virus. To test this hypothesis, both virus preparations were micro-infused bilaterally into the lateral amygdala ~3 days before tone fear conditioning5. Memory for tone conditioning was assessed by measuring the percentage of time the mice spent freezing during a tone presentation conducted 24 h after conditioning. To test the impact of inactivating transfected neurons, AL (10 μM, 0.5 μl) or vehicle were infused bilaterally into the lateral amygdala ~30 min before the retrieval of auditory fear memory. Remarkably, mice with HSV-CREB transfections (HSV-CREB mice) treated with AL showed less freezing (41.4% ± 3.7%, $t = 2.58$, $P < 0.05$) than HSV-CREB mice treated with saline (65.3% ± 8.5%), while AL had no effect on freezing of the HSV-LacZ mice (Supplementary Fig. 3).

As a control we also infused AL or vehicle into the lateral amygdala of separate groups of mice and waited 4 h (instead of 30 min) before testing tone conditioning (Supplementary Fig. 4). Our results showed that AL infusion 4 h before testing had no effect on retrieval, indicating that the effect of AL *in vivo* lasts at least 30 min, but no longer than 4 h. Additionally, the absence of a memory effect in mice that received the control virus strongly suggests that AL did not have a non-specific impact on lateral amygdala neuronal function. Thus, these data support the hypothesis that neurons with higher CREB function are disproportionally engaged in the neuronal representation that encodes tone fear memory in the lateral amygdala.

To test whether the effects of AL are reversible, we repeated the experiment just described, but this time added a second test 24 h after the first test. In the second test we reversed the treatments so that mice that got AL in the first test got VEH in the second test (and vice-versa). The results (Fig. 2a) show that the effects of AL were fully reversible, since HSV-CREB mice treated with AL in the first test (test 1, 50.7% ± 5.7% freezing) showed normal freezing in the second test (test 2, 67.1% ± 5.1%, $t = 2.14$, $n = 15$, $P < 0.05$) when treated with saline. Additionally, HSV-CREB mice treated with saline in the first test (71.1% ± 4.8% freezing) showed a memory impairment (freezing time 47.3% ± 5.8%, $t = 3.17$, $n = 17$, $P < 0.01$ compared to test 1) when treated with AL in the second test.

If higher CREB function increases the probability that neurons in the lateral amygdala encode the tone memory5, then inactivating those neurons during tone conditioning should

prevent them from participating in the encoding process, and consequently preclude HSV-CREB from biasing memory allocation. To test this hypothesis, we included an AL manipulation during both training and testing (Fig. 2b). Consistent with CREB's role in memory consolidation13,14, we found that activation of the HSV-CREB neurons during training enhanced tone-associated fear memory (VEH/VEH, 70.0% ± 5.5%, $n = 12$); while inactivation of the HSV-CREB neurons with AL during training reduced tone-associated fear memory to control levels (Fig. 2b, AL/VEH, 47.4% ± 6.4%, $n = 12$). More importantly, we found that although AL during testing disrupted freezing in mice that received saline during training (VEH/AL versus VEH/VEH), the same treatment did not affect freezing in mice that received AL during training (Fig. 2b, AL/AL, 49.5% ± 6.6%; AL/VEH, 47.4% ± 6.4%, $n = 12$ per group, Fisher's PLSD, $P > 0.05$). This result demonstrates that AL administration during testing does not affect memory retrieval in mice treated with AL during training, suggesting that HSV-CREB can only affect memory allocation when transfected cells are active during training. Altogether, these results indicate that neuronal activation during training is crucial for CREB's role in memory allocation.

Since our measures of memory allocation were taken at least 24 h after training (Fig. 2a–b), it is possible that the well known effects of CREB on memory consolidation13,14 could be confounding our interpretation of CREB's role on memory allocation. Thus, we tested memory allocation 30 min after training, a time point known to precede memory consolidation13,14. Indeed, when tested 30 min post-training, HSV-CREB mice did not show higher freezing than HSV-LacZ mice, demonstrating that HSV-CREB does not enhance tone fear memory 30 min post-training (Fig. 2c). Nevertheless, local administration of AL immediately after training did disrupt 30-min memory for tone conditioning in HSV-CREB mice (HSV-CREB/VEH, 50.9% ± 5.5%, HSV-CREB/AL, 28.9% ± 5.2%, $F_{3,44} = 6.93$, Fisher's PLSD, $P < 0.05$, $n = 12$ per group), while having no effect on HSV-LacZ mice (HSV-LacZ/VEH, 48.1% ± 7.5%, HSV-LacZ/AL, 52.9% ± 5.7%, Fig. 2c). These findings demonstrate that CREB's role in memory allocation cannot be attributed to its effects on memory consolidation. Additionally, these findings suggest that memory allocation can be observed as early as 30 min following training. Previous results suggested that transfection with HSV-CREB does not recruit more lateral amygdala neurons during encoding, and that the total number of lateral amygdala neurons involved in a specific memory remains unchanged across various CREB manipulations5,6. This implies that our tone fear results 24 h after training are not simply due to silencing of neurons driven into the amygdala memory trace by HSV-CREB.

To test the behavioral specificity of the HSV-CREB effects on memory, we repeated the experiments described above with two important modifications: First, we fear conditioned the mice *before* (and not after) viral injection. Then, we trained the same mice on taste aversion conditioning (CTA) 3 days following viral infection (Fig. 3). We chose CTA because it also depends on the amygdala15–17. As predicted, we found that AL infusion impaired CTA memory (Fig. 3b, HSV-CREB/VEH, 71.9% ± 7.7%, HSV-CREB/AL, 50.0% ± 5.9%, $t = 2.31$, $P < 0.05$) but had no effect on tone fear memory (Fig.3c, HSV-CREB/VEH, 50.6% ±8.6 %, HSV-CREB/AL, 49.9% ± 9.8%, $P > 0.05$). Importantly, the total levels of fluid consumption in CTA test were same in different treatment groups. These data

demonstrate the behavioral specificity of the HSV-CREB effects and also show that pre-, but not post-, training HSV-CREB infusions affect memory allocation in lateral amygdala. Importantly, these data also demonstrate that CREB has a role in the allocation of memory for CTA, suggesting that our findings may be generally applicable to amygdala-dependent learning.

HSV-CREB neurons show increased synaptic efficacy

Previous studies in thalamo-LA synapses following tone fear conditioning revealed increases in synaptic transmission and decreases in paired pulse facilitation (PPF)18,19. To test whether HSV-CREB neurons in lateral amygdala are preferentially recruited to encode fear memory, we studied synaptic transmission and PPF in HSV-CREB neurons and non-transfected neighboring cells in the same slices in both naive and conditioned mice (24 hrs post-training). Consistent with previous findings18,19 our whole-cell recording studies in the thalamo-LA pathway show that fear conditioning potentiates synaptic transmission (Fig. 4a left, two-way ANOVA, $F_{1,37} = 7.68$; $P < 0.01$) and decreases PPF (Fig.4a right, two-way ANOVA, $F_{1,82} = 26.35$; $P < 0.001$).

Importantly, we found that HSV-CREB neurons in conditioned mice (conditioned HSV-CREB) have both enhanced synaptic transmission and reduced PPF when compared with the other three control groups, including neighboring neurons without viral transfection in conditioned mice (conditioned CON), HSV-CREB neurons (naive HSV-CREB) and neighboring non-transfected neurons (naive CON) in naive mice (Fig.4b, One-way Repeated Measures ANOVA, $P < 0.001$). Statistical analysis showed that the evoked EPSCs and PPF in conditioned HSV-CREB neurons are significantly different from the other three groups (Newman-Keuls Multiple Comparison Test, $P < 0.001$). On the contrary, although the evoked EPSCs in conditioned CON neurons are also different from naive HSV-CREB and naive CON neurons ($P < 0.05$~0.01), the average PPFs among those three groups are identical ($P > 0.05$). Both synaptic EPSCs and PPF are indistinguishable in the naive HSV-CREB and naive CON groups, indicating that HSV-CREB did not change evoked basal synaptic transmission and PPF at thalamo-LA synapses in naive, unconditioned mice. Taken together, these data provide compelling additional evidence for the hypothesis that neurons with higher CREB function are disproportionally engaged in neuronal representations that encode tone fear memory in the lateral amygdala.

HSV-CREB neurons show increased neuronal excitability

How could neurons with higher CREB levels bias memory allocation? It is possible that higher levels of CREB lead to increased expression of specific channels and signaling proteins that increase the excitability of these neurons20–22, thereby increasing the probability that they are recruited during learning. To test this hypothesis, we prepared acute lateral amygdala slices ~3 days after virus infusion and performed whole-cell recordings. We found that although HSV-CREB did not affect the resting membrane potential, input resistance, spike amplitude or the spike half-width of transfected lateral amygdala pyramidal neurons (Supplementary Table), it did significantly lower the AP threshold of those neurons (Supplementary Table, HSV-CREB, −38.8 ± 0.9 mV, one-way ANOVA, $P < 0.05$ compared to the other three control groups, −35.4 ± 1.0 mV~ −35.7 ± 1.0 mV). In addition, HSV-

CREB caused a robust increase in the number of action potentials elicited by depolarizing current injections: in HSV-CREB neurons (n = 58, from 8 mice), the number of action potentials triggered by depolarizing current injections was higher than in non-transfected neurons or in neurons transfected with the HSV-LacZ control virus (Repeat ANOVA analysis, $P < 0.05$, Fig. 5a). Accordingly, HSV-CREB neurons showed a reduced spike-frequency adaptation: analysis of the distribution of neuronal firing properties indicated that 62% (36/58) of HSV-CREB neurons fired more than 6 spikes in response to a 400 pA, 600 ms current injection, while only 19% (12/64) of control neurons did so (Fig. 5b). Altogether, the decreased spike threshold, increased number of APs and reduced spike frequency adaptation indicate that HSV-CREB neurons have increased intrinsic excitability. Since the afterhyperpolarization (AHP) is also known to affect excitability23–27, we measured the post-burst AHP of HSV-CREB and control neurons at two time points: at the negative peak and 300 ms after the end of the current pulse. We found that HSV-CREB neurons have a significant reduction in the amplitude of the AHP measured at 300 ms after the current pulse, but not at peak amplitude (Fig. 5c), suggesting that later components of the AHP may be specifically affected by HSV-CREB.

Next, we determined whether the intrinsic excitability changes in HSV-CREB neurons alter the input-output function of neurons, a critical property for information processing during learning. We measured the relationship between the EPSP slope and spike probability following different synaptic stimulation intensities (the E-S curve) in HSV-CREB transfected and neighboring control neurons. We observed a leftward shift of the E-S curve in HSV-CREB neurons (Fig. 6, HSV-CREB, 2.6 ± 0.3 mV ms^{-1}, CON, 4.6 ± 0.6 mV ms^{-1}, $P < 0.01$). Specifically, we found a decrease in the EPSP slope that yields action potentials with 50% probability, which can be explained by a lower threshold for action potential generation in HSV-CREB cells (Supplementary Table). In contrast, the slope of the E-S curve was not changed. This result indicates that HSV-CREB neurons have stronger EPSP-spike coupling.

Previous studies showed that both changes in synaptic strength (LTP) and changes in intrinsic excitability could lead to a left shift of the E-S curve28–30. Our whole-cell recordings in HSV-CREB and neighboring non-transfected neurons showed that HSV-CREB did not change evoked basal synaptic transmission and PPF at thalamo-LA synapses in naive mice (Fig. 4b). Additionally, there is no detectable difference in AMPA/NMDA EPSC ratio between HSV-CREB and HSV-LacZ neurons (Supplementary Fig.5). Consistently, HSV-CREB expression did not change the slope of the E-S curve (Fig.6), suggesting that inhibition is not changed28–30. Thus, in our study, the E-S potentiation observed in HSV-CREB neurons is likely due to changes in the intrinsic electrical properties of postsynaptic neurons. All together, our analyses of intrinsic and synaptically driven excitability in naïve mice demonstrate that HSV-CREB increases the excitability of lateral amygdala neurons and strengthen their input-output function. These findings provide a possible explanation for the selective role of CREB in memory allocation: neurons with higher CREB levels have higher excitability and therefore are more likely to be recruited in a memory trace.

DISCUSSION

With a novel approach, we demonstrate here that CREB can modulate the allocation of fear memory to specific neurons in the lateral amygdala, and that neuronal excitability may play a key role in this process. Since we showed that neurons with the viral encoded CREB (i.e. higher CREB levels) are more excitable, they are more likely to be both activated during conditioning and recruited into storing the conditioning episode. Synchronous or correlated activity with thalamic inputs could in turn lead to the strengthening of thalamo-amygdala connections with these neurons. Indeed, our findings showed that these synapses are stronger in HSV-CREB neurons from trained mice. Thus, only a specific subset of neurons, the ones with higher levels of CREB and therefore higher excitability, will be engaged in the memory trace.

Besides a role in excitability, a large body of evidence indicates that CREB-dependent transcription is essential for both long-lasting forms of synaptic plasticity and long-term memory, but not short-term plasticity or short-term memory31–35. Thus, the excitability and synaptic plasticity mediated by CREB will eventually work together to support the memory representation in a subset of neurons of the lateral amygdala.

It is possible that differences in the endogenous levels of CREB activity normally contribute to the diversity of firing properties in projection neurons in the lateral amygdala24. Although the CREB target genes that are responsible for changes in excitability in lateral amygdala neurons described above are still not known, it is possible that, as previously shown in other brain areas20–22, 36, higher CREB levels/activity in the amygdala change the expression of voltage-dependent ion channels, as well as second messenger systems that modulate those channels, and consequently increase the excitability of specific amygdala neurons37. This subset of neurons with higher excitability could then be more easily activated during learning and would therefore be more likely to be recruited into specific memory representations. Thus, dynamic regulation of intracellular CREB activity in individual neurons of a network might be one of the crucial organizing principles for memory allocation. Therefore, some or all of the cooperating and antagonizing signaling pathways known to regulate CREB activity might fine tune the process that allocates memories in neuronetworks37.

Following robust activation of CREB, it is also possible that CREB repressors, such as ICER (inducible cAMP early repressor)38, are transcribed. The progressive accumulation of CREB repressors could then have an overall negative impact on CREB activity and therefore on memory allocation. The balance of factors that either promote or dampen neuronal excitability would then control whether two memories are stored in the same or different cells. It is possible that CREB is only one of many factors involved in memory allocation, and that excitability is just one of several mechanisms that determine which cells in a network encode a given memory.

Our results provide direct evidence that memory is not evenly stored in neuronal networks1, 2, 5, 6, and that CREB has a role in determining which subset of neurons is recruited during training. Notably, CREB does not seem to change the total number of neurons in the

memory trace5,6, suggesting that there may be a competitive process that determines cellular participation in the memory trace. At a circuit level, it is possible that there is a relationship between the total number of activated neurons and network inhibition; the initial recruitment of a larger number of neurons would result in stronger inhibition and therefore in a feedback circuit process that limits the total number of cells committed to any one given memory.

The results reported here, together with other recent related studies5,6, represent an important step towards unraveling the organizing principles and mechanisms behind the emergence of Hebbian cell assemblies responsible for information storage and retrieval in brain structures such as the amygdala.

ONLINE METHODS

Mice

Adult F_1 hybrid (C57Bl/6NTac × 129S6/SvEvTac) mice were group-housed (three to four per cage) on a 12 h light/dark cycle. Food and water were available ad libitum throughout the experiment. All procedures were approved by the Chancellor's Animal Research Committee at the University of California at Los Angeles, in accordance with National Institutes of Health guidelines.

HSV vectors

Two vectors were used, HSV-CREB-AlstR (HSV-CREB vector) and HSV-LacZ-AlstR (Control vector). Genes of interest (*Creb1*, *LacZ* and *AlstR*) were cloned into a bicistronic HSV amplicon7. To visualize transgene expression, we fused eGFP to the 5′ end of the CREB and LacZ cDNA. CREB or LacZ is expressed from an IE 4/5 promoter and AlstR from a CMV promoter. The amplicon was packaged according to published methods39.

Surgery and virus infusion

Mice were pretreated with atropine sulfate (0.1 mg kg^{-1}, i.p.), anesthetized with chloral hydrate (400 mg kg^{-1}, i.p.), and placed in a stereotaxic frame. The skin was retracted and holes drilled in the skull bilaterally above the LA (AP = −1.3, ML = ± 3.3, V = − 4.8 mm from bregma) according to Paxinos and The Franklin mouse brain atlas40. For behavioral experiments, a stainless steel outer cannula (Plastic One) was implanted to LA and fixed on the skull with dental cement. After cannula implantation, mice were single-housed and handled every day. Virus infusion was delayed until seven days after surgery to ensure physical recovery. A virus solution (1.3 μl; bilateral) was delivered to lateral amygdala at a flow rate of 0.065 μl/min through inner injection cannula (Plastic one, 22 gauge) attached by polyethylene tubing to Hamilton microsyringes mounted in an infusion pump (Harvard Instruments). The infusion cannula was left in place an additional 10 min to ensure diffusion of the vector. For electrophysiological studies, virus solution (1.3 μl) was delivered to LA over 5 min through glass micropipettes (Sutter Instrument) immediately after the holes were drilled. The micropipette was left in place for 5 min post-injection. Electrophysiological or behavioral experiments were performed 3 days following virus infusion41.

AL administration

The peptide allatostatin (AL)12 (New England) was dissolved in ddH_2O to make a 2.5 mM stock solution. Saline was added to dilute it to the proper final concentration for each specific experiment. AL solution (0.5 μl) or same amount of vehicle (saline) was delivered bilaterally to the LA of awake animals at a flow rate of 0.25 μl/min through inner injection cannula. The cannula was left in place for 2 min post-injection. Behavioral procedures were started ~30 min after injection.

Auditory (tone) fear conditioning

Training consisted of placing the mice in a conditioning chamber (Context A) and 2 min later presenting a tone (2800 Hz, 85 dB, 30 sec) that co-terminated with a shock (2 sec, 0.5 mA). Mice remained in the chamber for an additional 1 min. Test for auditory fear conditioning occurred either 30 min or 24 h later. Mice were placed in a novel chamber (Context B) and 2 min later the tone CS was presented (for 1 min). Our index of memory, freezing (the cessation of all movement except for respiration), was assessed via an automated scoring system (Med Associates Inc.) with a 30 frames/sec sampling; the animals needed to freeze continuously for at least 1 sec before freezing could be counted. The same training protocol was also used in the electrophysiological studies. Slices were cut 24 h after training.

Conditioned taste aversion (CTA)

CTA training took place in the light part of the cycle 7 days following surgery. Mice were water deprived for 24 h and then pretrained for 5 days to get their daily water ration within 40 min per day from two tubes (10 ml). Three hours after the 2nd day pretraining, HSV virus was infused into LA on both sides. Conditioning day started 3 days after virus injection.

On the conditioning day, the two tubes were filled with 0.2% saccharin sodium salt (w/v, the taste CS) instead of water. The CS was presented for 20 min and 20 min later, mice were treated with the malaise inducing agent lithium chloride (LiCl; 0.06 M, 2% body weight i.p.).

Testing for aversion to saccharin occurred 24 h later. AL/vehicle was infused 30min before testing. Two tubes (one contains water and the other contains saccharin) were presented for 40 min. The intake of each fluid was measured and the aversion index (AI) was defined as follows: [milliliters of water consumed/(milliliters of water + milliliters of saccharin consumed)]×100%. 50% AI is equal preference level, and the higher the AI, the more the mice prefer water to saccharin).

Histology

After the behavioral experiments, mice were perfused transcardially with 4% paraformaldehyde in 0.1M phosphate buffer, pH 7.4. Brains were sliced coronally (40 μm). The cannula tip locations were confirmed by crystal violet staining at the end of each experiment. Only those mice with bilateral placements in the basolateral complex of the amygdala were included in analysis.

Quantitative analyses of infection levels were performed using the NIH Image processing system. Before confocal imaging we used transmission light microscopy and the thalamo-lateral amygdala fibers (ic) and the cortico-lateral amygdale fibers (oc) to locate the dorsal and lateral boundary of LA. The total number of GFP-positive cells in the LA was counted bilaterally with a fixed sample window (0.1 mm^2) across at least six sections from comparable anteroposterior levels from each mouse. To assess the number of nuclei in the areas counted, the slices were re-stained using 4',6'-diamidino-2-phenylindole (DAPI) after washout of FITC-conjugated GFP primary antibody. The percentage of GFP positive cells was calculated as the percentage of GFP-positive cell/total DAPI-labeled nuclei in the LA. After the immunofluorescent studies, brain slices were counter stained with crystal violet to confirm the position of the infusion cannula.

Electrophysiology

Two to three days after virus infusion, brains were rapidly removed from adult mice (3 to 4 months old) and placed in ice cold artificial cerebral spinal fluid (ACSF) containing (in mM): 120 NaCl, 20 $NaHCO_3$, 3.5 KCl, 1.25 NaH_2PO_4, 2.5 $CaCl_2$, 1.3 $MgSO_4$, and 10 d-glucose. Coronal slices (400 μm thick) containing the amygdala were prepared and allowed to recover in oxygenated (95% O_2 / 5% CO_2) ACSF at room temperature for at least 1 h before experiments were performed. All solutions were bubbled with 95% O_2 / 5% CO_2 and perfused over the slice at a rate of ~2 ml/min at 31°C. Cells were visualized with an upright microscope using infrared or epifluorescent illumination, and whole-cell current-clamp recordings were made from neurons in the LA with a Dagan 3900A amplifier and Multiclamp 700A. Electrodes (3~6 MΩ) contained in mM: 120 K-methansulfate, 20 KCl, 10 HEPES, 0.2 EGTA, 2.0 $MgCl_2$, 2 Mg_2ATP, 0.3 Na_3GTP, 7 phosphocreatine (pH 7.2~7.4; 290~300 mOsm). Alexa 568 (0.2 mg ml^{-1}, Molecular Probes, OR) was included in the internal solution. Responses were filtered at 2 kHz and digitized at 10 kHz. All data were acquired, stored, and analyzed using pClamp9.0 (Axon Instruments) and Matlab (R2007a). Access resistance was monitored throughout the experiment. Input resistance was monitored throughout the experiment by applying a hyperpolarizing current (−100 pA). Only cells that reached the minimal criteria for health and stability (resting membrane potential more negative than −55 mV and access resistance less than 20 MΩ) were included in the analyses of this study. Pyramidal neurons in LA were identified based on their action potential (AP) half width and spike frequency adaptation in response to a long depolarizing current injection, as describe previously24. Cell passive membrane properties were examined at resting potential (RP). The spike amplitude, half-width and spike threshold were measured from the first spike in each trace that showed the smallest number of evoked spikes (usually only 1 spike) in response to a depolarizing step (either 50,100 or 150 pA, 600 ms). Spike amplitudes were measured from RP. The threshold for spike initiation was taken as the beginning of the upstroke of the AP. AP half-widths were measured as the spike width at the half-maximal voltage. Input resistance was calibrated by fitting the I-V curve with linear regression. To investigate the firing properties of neurons, fifteen current injection steps (600 ms in duration) were delivered from −200 to 500 pA in 50 pA increments. This protocol was repeated three times to obtain stable responses. As for the AL experiments, this protocol was repeated six times, two to obtain control responses, two after the application of AL and two repeated again after washout of AL. The LA cells recorded were further divided

into two groups based on spike-frequency adaptation24: Rapidly adapting (RA) cells fired only 1–5 spikes at the onset of the current injection (600 ms, 400 pA) and remained silent for the rest of the current pulses. Slowly adapting (SA) cells fired more than 6 spikes. Post-burst afterhyperpolarizations (AHP) were evoked in current clamp by applying a 50 ms, supra-threshold stimulation (≥400 pA, mostly 400pA) current step from a holding potential of −60 mV to induce at least 2 spikes42, 43. Cells fire only once with varying injection currents are excluded from further analysis. The AHPs were measured at two time point: the negative peak of the AHP and 300 ms after the end of the 50 ms pulse. Drugs were applied by adding them to the superfusate at the appropriate concentration. Since the neuronal excitability of uninfected cells in HSV-CREB mice (n = 40, 8 mice), HSV-LacZ vector transfected cells (n = 12, 2 mice) and nearby uninfected cells (n = 12, 2 mice) were not significantly different (P > 0.05), we pooled the data and used it as a control.

The thalamo-LA pathway was stimulated with a bipolar platinum electrode. The distance between the recording and stimulating sites was between 150 and 450μm. 100us stimuli were delivered at 10 s intervals. For the basal synaptic transmission studies, the input-output curve was constructed by varying stimulus intensity (10 to 100μA) and measuring corresponding EPSC amplitude. Peak EPSC was measured as the peak inward current. For paired-pulse facilitation (PPF) studies, the peak amplitude for individual responses was measured as the difference between the current level before the stimulus artifact and the peak of the EPSC18. Stimulation position and intensity were set to evoke an EPSC of ~50–200 pA. As for experiments carried on trained animals, the same training protocol (see description in tone fear conditioning part) was applied and recordings were conducted 24 h after training.

To compare the AMPA/NMDA ratio of evoked synaptic transmission, the AMPA component was measured as the EPSC peak amplitude at −70 mV; the NMDA component was determined by measuring the current amplitude at 100 ms after EPSC onset at 30 mV44. Stimulation position and intensity were set to evoke an EPSC of ~50–200 pA. In the AMPA/NMDA ratio study, experiments were performed in the presence of the $GABA_A$ receptor blocker picrotoxin (100 μM).

For synaptically evoked excitability studies, a series of pulses (at least 60 pulses, 10 pulses for each stimulation intensity) were given at each of the stimulation intensities used (covering a range of responses from subthreshold to supramaximal). E-S curves were constructed by binning the totality of the EPSP slopes and plotting the average of the bin versus the percentage of successful action potentials in that bin29. Stimulation intensities ranged from 30 to 300 μA. The data points were fit with a sigmoid: $S = 1/(1+ \exp[(E50-E)/K])$, where E50 is the EPSP slope that yields action potentials 50% probability (the I/O threshold). The gain was determined by calculating the slope of the linear potion of the sigmoid.

Statistical analysis

Results are expressed as mean ± SEM. ANOVA analyses or *t*-tests were used for statistical comparisons between groups as described in the context. P < 0.05 means significant difference between groups.

Supplementary Material

Refer to Web version on PubMed Central for supplementary material.

ACKNOWLEDGMENTS

We thank Tiago Carvalho, Yong-Seok Lee, Peyman Golshani, Dean Buonomano, Brian Wiltgen, Wenbin Tan, Justin Shobe, Jack Feldman and John Guzowski for helpful advice, Edward Callaway for AlstR cDNA, Katie Cai for technical support. This work was supported by grants from NIH (P50-MH0779720 and R37-AG13622) to AJS and a Marie Curie Outgoing fellowship of the European Commission (PIOF-GA-2008–219622) to PP.

REFERENCES

1. Repa JC, et al. Two different lateral amygdala cell populations contribute to the initiation and storage of memory. Nat Neurosci. 2001; 4:724–31. [PubMed: 11426229]
2. Rumpel S, LeDoux J, Zador A, Malinow R. Postsynaptic receptor trafficking underlying a form of associative learning. Science. 2005; 308:83–8. [PubMed: 15746389]
3. Reijmers LG, Perkins BL, Matsuo N, Mayford M. Localization of a stable neural correlate of associative memory. Science. 2007; 317:1230–3. [PubMed: 17761885]
4. Schafe GE, Doyere V, LeDoux JE. Tracking the fear engram: the lateral amygdala is an essential locus of fear memory storage. J Neurosci. 2005; 25:10010–4. [PubMed: 16251449]
5. Han JH, et al. Neuronal competition and selection during memory formation. Science. 2007; 316:457–60. [PubMed: 17446403]
6. Han JH, et al. Selective erasure of a fear memory. Science. 2009; 323:1492–6. [PubMed: 19286560]
7. Clark MS, et al. Overexpression of 5-HT1B receptor in dorsal raphe nucleus using Herpes Simplex Virus gene transfer increases anxiety behavior after inescapable stress. J Neurosci. 2002; 22:4550–62. [PubMed: 12040062]
8. Birgul N, Weise C, Kreienkamp HJ, Richter D. Reverse physiology in drosophila: identification of a novel allatostatin-like neuropeptide and its cognate receptor structurally related to the mammalian somatostatin/galanin/opioid receptor family. Embo J. 1999; 18:5892–900. [PubMed: 10545101]
9. Karschin C, Dissmann E, Stuhmer W, Karschin A. IRK(1–3) and GIRK(1–4) inwardly rectifying K^+ channel mRNAs are differentially expressed in the adult rat brain. J Neurosci. 1996; 16:3559–70. [PubMed: 8642402]
10. Tan EM, et al. Selective and quickly reversible inactivation of mammalian neurons *in vivo* using the Drosophila allatostatin receptor. Neuron. 2006; 51:157–70. [PubMed: 16846851]
11. Tan W, et al. Silencing preBotzinger complex somatostatin-expressing neurons induces persistent apnea in awake rat. Nat Neurosci. 2008; 11:538–40. [PubMed: 18391943]
12. Lechner HA, Lein ES, Callaway EM. A genetic method for selective and quickly reversible silencing of Mammalian neurons. J Neurosci. 2002; 22:5287–90. [PubMed: 12097479]
13. Kida S, et al. CREB required for the stability of new and reactivated fear memories. Nat Neurosci. 2002; 5:348–55. [PubMed: 11889468]
14. Bourtchuladze R, et al. Deficient long-term memory in mice with a targeted mutation of the cAMP-responsive element-binding protein. Cell. 1994; 79:59–68. [PubMed: 7923378]
15. Yamamoto T, Shimura T, Sako N, Yasoshima Y, Sakai N. Neural substrates for conditioned taste aversion in the rat. Behav Brain Res. 1994; 65:123–37. [PubMed: 7718144]
16. Lamprecht R, Hazvi S, Dudai Y. cAMP response element-binding protein in the amygdala is required for long- but not short-term conditioned taste aversion memory. J Neurosci. 1997; 17:8443–50. [PubMed: 9334416]
17. Josselyn SA, Kida S, Silva AJ. Inducible repression of CREB function disrupts amygdala-dependent memory. Neurobiol Learn Mem. 2004; 82:159–63. [PubMed: 15341801]
18. McKernan MG, Shinnick-Gallagher P. Fear conditioning induces a lasting potentiation of synaptic currents *in vitro*. Nature. 1997; 390:607–11. [PubMed: 9403689]

19. Huang YY, Kandel ER. Postsynaptic induction and PKA-dependent expression of LTP in the lateral amygdala. Neuron. 1998; 21:169–78. [PubMed: 9697861]
20. Han MH, et al. Role of cAMP response element-binding protein in the rat locus ceruleus: regulation of neuronal activity and opiate withdrawal behaviors. J Neurosci. 2006; 26:4624–9. [PubMed: 16641242]
21. Dong Y, et al. CREB modulates excitability of nucleus accumbens neurons. Nat Neurosci. 2006; 9:475–7. [PubMed: 16520736]
22. Viosca J, Lopez de Armentia M, Jancic D, Barco A. Enhanced CREB-dependent gene expression increases the excitability of neurons in the basal amygdala and primes the consolidation of contextual and cued fear memory. Learn Mem. 2009; 16:193–7. [PubMed: 19237641]
23. Murphy GG, et al. Increased neuronal excitability, synaptic plasticity, and learning in aged Kvbeta1.1 knockout mice. Curr Biol. 2004; 14:1907–15. [PubMed: 15530391]
24. Faber ES, Callister RJ, Sah P. Morphological and electrophysiological properties of principal neurons in the rat lateral amygdala *in vitro*. J Neurophysiol. 2001; 85:714–23. [PubMed: 11160506]
25. Storm JF. Potassium currents in hippocampal pyramidal cells. Prog Brain Res. 1990; 83:161–87. [PubMed: 2203097]
26. Oh MM, McKay BM, Power JM, Disterhoft JF. Learning-related postburst afterhyperpolarization reduction in CA1 pyramidal neurons is mediated by protein kinase A. Proc Natl Acad Sci U S A. 2009; 106:1620–5. [PubMed: 19164584]
27. Santini E, Quirk GJ, Porter JT. Fear conditioning and extinction differentially modify the intrinsic excitability of infralimbic neurons. J Neurosci. 2008; 28:4028–36. [PubMed: 18400902]
28. Staff NP, Spruston N. Intracellular correlate of EPSP-spike potentiation in CA1 pyramidal neurons is controlled by GABAergic modulation. Hippocampus. 2003; 13:801–5. [PubMed: 14620875]
29. Carvalho TP, Buonomano DV. Differential effects of excitatory and inhibitory plasticity on synaptically driven neuronal input-output functions. Neuron. 2009; 61:774–85. [PubMed: 19285473]
30. Losonczy A, Makara JK, Magee JC. Compartmentalized dendritic plasticity and input feature storage in neurons. Nature. 2008; 452:436–41. [PubMed: 18368112]
31. Silva AJ, Kogan JH, Frankland PW, Kida S. CREB and memory. Annu Rev Neurosci. 1998; 21:127–48. [PubMed: 9530494]
32. Shaywitz AJ, Greenberg ME. CREB: a stimulus-induced transcription factor activated by a diverse array of extracellular signals. Annu Rev Biochem. 1999; 68:821–61. [PubMed: 10872467]
33. Mayr B, Montminy M. Transcriptional regulation by the phosphorylation-dependent factor CREB. Nat Rev Mol Cell Biol. 2001; 2:599–609. [PubMed: 11483993]
34. Lonze BE, Ginty DD. Function and regulation of CREB family transcription factors in the nervous system. Neuron. 2002; 35:605–23. [PubMed: 12194863]
35. Carlezon WA Jr. Duman RS, Nestler EJ. The many faces of CREB. Trends Neurosci. 2005; 28:436–45. [PubMed: 15982754]
36. Jancic D, Lopez de Armentia M, Valor LM, Olivares R, Barco A. Inhibition of cAMP Response Element-Binding Protein Reduces Neuronal Excitability and Plasticity, and Triggers Neurodegeneration. Cereb Cortex. 2009
37. Won J, Silva AJ. Molecular and cellular mechanisms of memory allocation in neuronetworks. Neurobiol Learn Mem. 2008; 89:285–92. [PubMed: 17962049]
38. Sassone-Corsi P. Transcription factors responsive to cAMP. Annu Rev Cell Dev Biol. 1995; 11:355–77. [PubMed: 8689562]
39. Lim, F.; Neve, RL. R.L. Curr Protoc Neurosci. Greene Publishing Assoc. and Wiley-Interscience; New York: 1999.
40. Paxinos, G.; Franklin, KBJ. The mouse brain in stereotaxic coordinates. Academic Press; San Diego: 2003.
41. Barrot M, et al. CREB activity in the nucleus accumbens shell controls gating of behavioral responses to emotional stimuli. Proc Natl Acad Sci U S A. 2002; 99:11435–40. [PubMed: 12165570]

42. Faber ES, Sah P. Opioids inhibit lateral amygdala pyramidal neurons by enhancing a dendritic potassium current. J Neurosci. 2004; 24:3031–9. [PubMed: 15044542]
43. Liebmann L, et al. Differential effects of corticosterone on the slow afterhyperpolarization in the basolateral amygdala and CA1 region: possible role of calcium channel subunits. J Neurophysiol. 2008; 99:958–68. [PubMed: 18077660]
44. Humeau Y, et al. A pathway-specific function for different AMPA receptor subunits in amygdala long-term potentiation and fear conditioning. J Neurosci. 2007; 27:10947–56. [PubMed: 17928436]

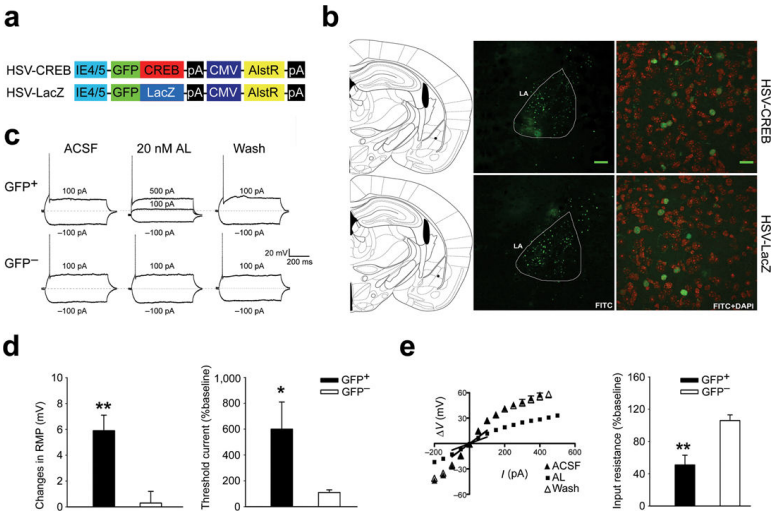

Fig. 1.

Selective and reversible modulation of a set of genetically targeted LA neurons. (**a**) Schematic of the viral amplicons. (**b**) Robust and localized GFP expression in LA following HSV-CREB (top) and HSV-LacZ virus infection (bottom). Left: illustration of cannula tip locations (black dot in LA) of the representative brain slices (middle). Middle: low magnification images showing GFP expression (green) in LA following virus infection. Calibration bar: 120μm. Right: high magnification images showing GFP expression in LA neurons. Transfected LA cells were double-stained with GFP (green) and DAPI (red). Calibration bar: 20 μm. (**c**) Representative traces showing that AL (20 nM) quickly (~5 min) and reversibly inactivates transfected (GFP^+) LA pyramidal neurons, whereas it has no effect on neighboring non-transfected (GFP^-) neurons in the same slices. The dashed line indicates the resting potential at −60 mV. The currents injected are shown next to associated traces. (**d**) Summary of the selective effect of AL on resting membrane potential (RMP, left) and the spike current threshold (right) of transfected LA neurons. (**e**) The selective effect of AL on input resistance of transfected LA neurons. Left: IV curves and linear regression used to calibrate input resistance. Right: summary of the selective effects of AL. In **c–e**, the transfected neurons include both HSV-CREB and HSV-LacZ neurons. Only ~2 neurons were recorded from the same slice. n = 12~16 cells from 4 mice for each experimental group. Unpaired t test, $^*P < 0.05$ and $^{**}P < 0.01$ as indicated.

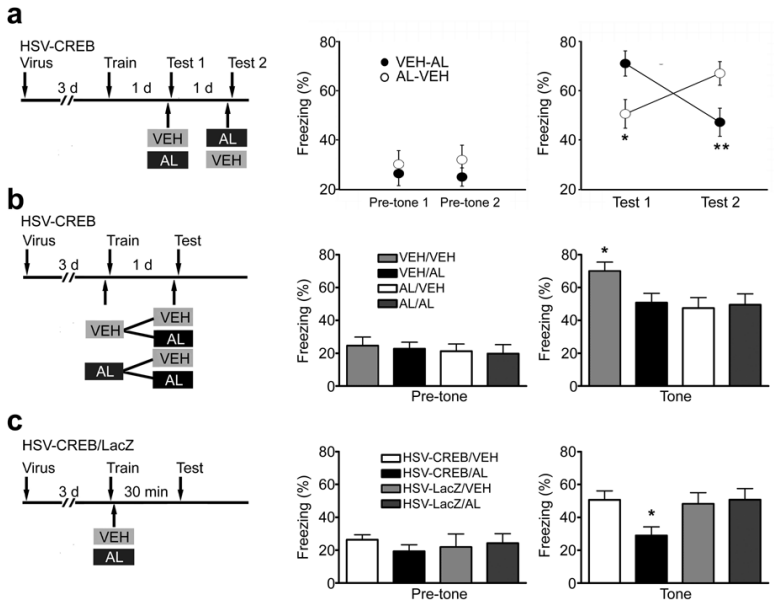

Fig. 2.

Local infusion of AL selectively impairs auditory fear memory in HSV-CREB mice. (**a–c**) Left: schematic of the experimental design. Middle: measurements of freezing before tone presentation (pre-tone); Right: measurements of freezing during tone presentation (tone). (**a**) Histogram showing that the effect of AL is reversible. Mice were tested twice (test 1 and test 2), 1 day apart. The VEH-AL group (n = 17) represents mice that received VEH during test 1 and AL during test 2. The AL-VEH group (n = 15) had the opposite treatment. ** $P < 0.01$ and *$P < 0.05$ as indicated. (**b**) Summary graph shows that although AL during testing impairs freezing in mice free of AL during training (VEH/AL versus VEH/VEH), it has no effect in mice that received AL during training (AL/AL versus AL/VEH). VEH/VEH or AL/AL represents mice that received VEH or AL both during training and testing. VEH (AL)/AL (VEH) represent VEH (AL) during training and AL (VEH) during testing. n = 12 mice for each experimental group. One way ANOVA, $F_{3,44} = 2.96$, Fisher's PLSD, *$P <$ 0.05 as indicated. (**c**) Histogram showing that AL selectively blocks short-term fear memory in HSV-CREB mice. Fisher's PLSD, *$P < 0.05$, n = 12 mice for each group.

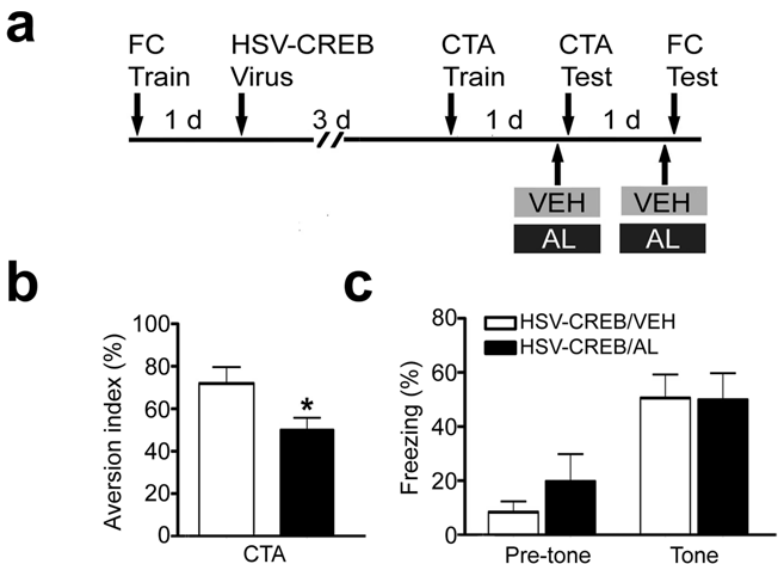

Fig. 3.

AL does not disrupt conditioning in HSV-CREB mice established prior to viral transfection. (**a**) Schematic of the experimental design. (**b**) Histogram showing that AL infusion impairs CTA memory, which was generated after virus infusion (training after virus infusion). The aversion index (AI) is defined as follows: [milliliters of water consumed / (milliliters of water + milliliters of saccharin consumed)] ×100%. The higher the AI, the more the mice prefer water to saccharin and the better the CTA memory. Unpaired *t* test, $*P < 0.05$ as indicated. (**c**) AL had no effect on established tone fear memory (training before virus infusion). Pre-tone: freezing before tone presentation. Tone: freezing during tone presentation. $n = 9$ mice for AL group and $n = 6$ for VEH group.

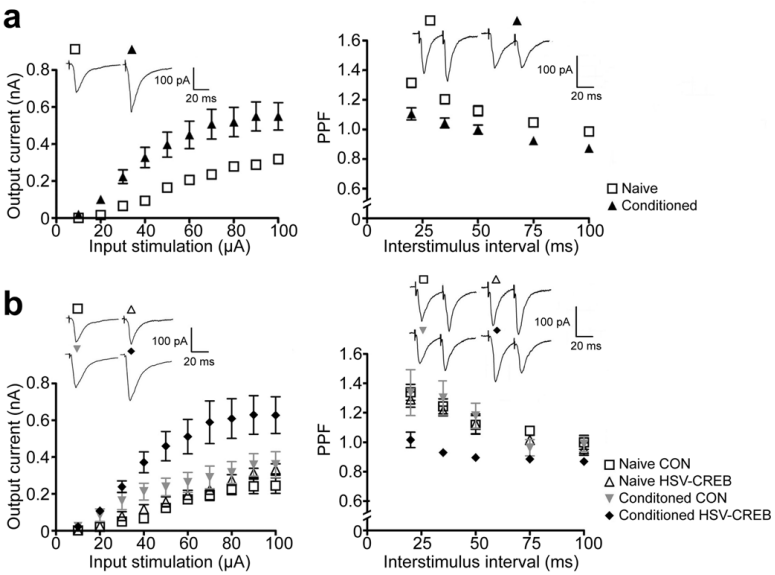

Fig. 4.

HSV-CREB neurons in conditioned mice show increased synaptic efficacy (**a**) Comparison of LA synaptic properties in naive versus conditioned mice. “Naive”, neurons in untrained mice; “Conditioned”, neurons in trained mice. Left: Evoked EPSCs in thalamo-LA synapses were enhanced after conditioning. Two-way ANOVA, $F_{1,37} = 7.68$; $P < 0.01$. Naive, $n = 15$; Conditioned, $n = 24$ from 6 mice per group. Right: PPF was decreased in thalamo-LA synapses after conditioning. Two-way ANOVA, $F_{1,82} = 26.35$; $P < 0.001$. Naive, $n = 37$; Conditioned, $n = 47$ from 8 mice per group. (**b**) Comparison of LA synaptic properties in naive versus conditioned mice transfected with HSV-CREB virus. “Naive CON” and “Conditioned CON” refer to non-transfected (GFP^-) LA neurons, whereas “Naive HSV-CREB” and “Conditioned HSV-CREB” refer to transfected (GFP^+) neurons from naive and conditioned mice. Left: HSV-CREB neurons ($n = 12$) show increased synaptic EPSCs after conditioning, compared with other groups (naive CON, $n = 5$; naive HSV-CREB, $n = 7$; conditioned CON, $n = 8$, from 5~6 mice per group). One-way Repeated ANOVA, $P < 0.001$, Newman-Keuls Multiple Comparison (NKMC) Test, $P < 0.001$. Right: HSV-CREB neurons show decreased PPF after conditioning. HSV-CREB neurons, $n = 13$; naive CON, $n = 10$; naive HSV-CREB, $n = 11$; conditioned CON, $n = 8$, from 6 mice per group. One-way ANOVA, $P < 0.001$, NKMC Test, $P < 0.001$. Inserts: sample traces from different neurons as indicated. The stimulation intensity is 30μA and the interstimulus interval in PPF is 35 ms.

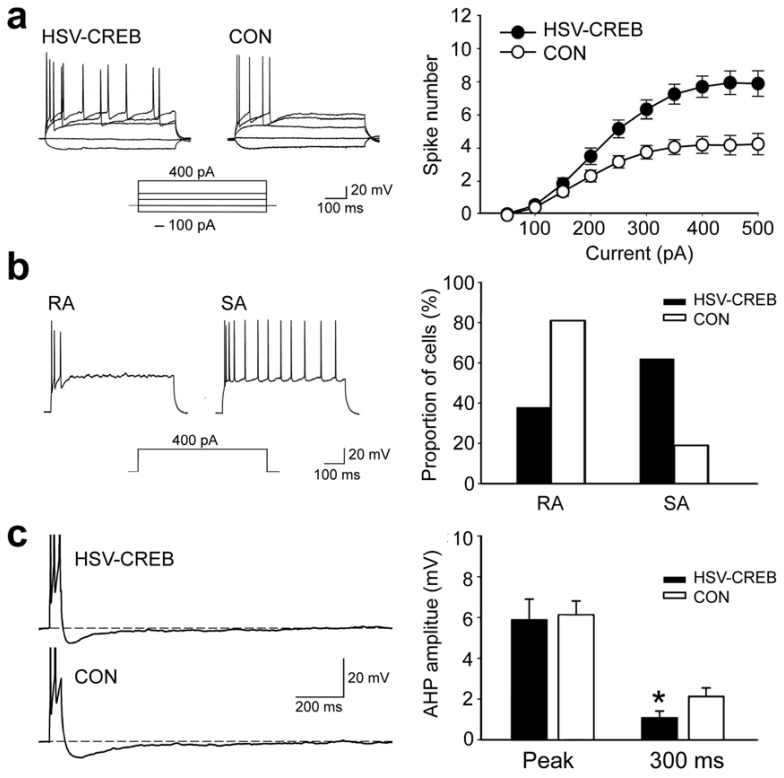

Fig. 5.

CREB increases neuronal excitability in transfected LA neurons. (**a**) Left: traces of sample recordings showing more APs in response to increasing current injections (−100, 0, 100, 200 and 400 pA; 600 ms) in a HSV-CREB neuron than in a neighboring non-transfected neurons (CON). Right: a plot of the number of evoked spikes as a function of injected current shows significantly more APs in HSV-CREB neurons (n = 58, from 8 mice) than in controls (*n* = 64, from 12 mice from the other three groups, Repeated ANOVA, $P < 0.05$). (**b**) HSV-CREB changed the firing properties of transfected LA pyramidal neurons. Left: sample voltage traces showing two LA neurons with distinct firing properties (RA and SA)24. Rapidly adapting (RA) cells fired only 1–5 spikes at the onset of the current injection (600 ms, 400 pA) and remained silent for the rest of the current pulses. Slowly adapting (SA) cells fire more than 6 spikes. Right: distribution of firing properties of HSV-CREB neurons and control LA neurons. (**c**) HSV-CREB neurons show reduced post-burst AHP compared to control neurons. Left: sample post-burst AHP traces from a HSV-CREB neuron and a neighboring control neuron. Right: histogram showing AHP difference between HSV-CREB neurons (*n* = 58, from 8 mice) and the control neurons (*n* = 64, from 12 mice from the other three groups) as measured at peak and 300 ms after the end of current step. Unpaired *t* test, $*P < 0.05$ as indicated.

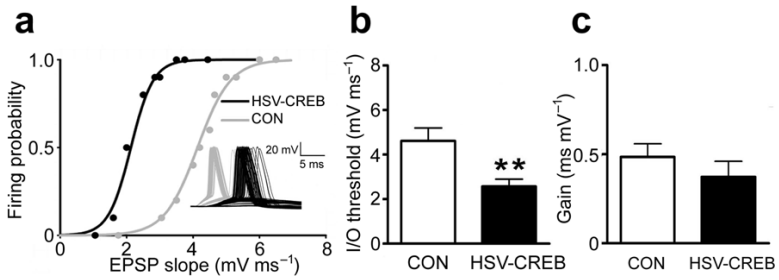

Fig. 6.

HSV-CREB changes the input-output function of transfected LA neurons. (**a**) Unit E-S curve of a HSV-CREB neuron and a neighboring non-transfected neuron (CON). Insert: representative EPSPs and action potentials traces from a HSV-CREB and a CON neuron following increasing synaptic stimulations. (**b**) Histogram showing that HSV-CREB lowers the inpu-output threshold in transfected LA neurons. The threshold was quantified as the EPSP slope ($mVms^{-1}$) corresponding to 50% firing probability. (**c**) Histogram showing that HSV-CREB does not change the slope (Gain) of the linear component of the E-S curve. HSV-CREB, $n = 10$ and CON, $n = 11$ from 5 mice. Unpaired t test, $^{*}P < 0.01$ as indicated.